Preprints of the 21st IFAC World Congress (Virtual)
Berlin, Germany, July 12-17, 2020

Lyapunov-based observer design for steam boilers

Stefan L. Hölzl [*,***] **Richard Seeber** [*,***] **Markus Tranninger** [**]
Robert Bauer [***] **Martin Horn** [*]

[*] *Christian Doppler Laboratory for Model Based Control of Complex Test Bed Systems, Institute of Automation and Control, Graz University of Technology, Graz, Austria. (e-mail:* stefan.hoelzl@tugraz.at*)*
[**] *Institute of Automation and Control, Graz University of Technology, Graz, Austria. (e-mail:* markus.tranninger@tugraz.at*)*
[***] *Kristl, Seibt & Co GmbH, Graz, Austria. (e-mail:* robert.bauer@ksengineers.at*)*

Abstract: Steam boilers are widely used in industrial applications ranging from air conditioning to power plants. Advanced control schemes for such boilers require the knowledge of internal state variables, which are not always measurable. This paper proposes a new observer for steam boilers whose construction builds on a special state variable choice and a Lyapunov-based design of the observer gains. Tuning insight is gained from an oscillator-like structure of the (linearised) observer error dynamics. Comparisons to an extended Kalman filter in simulations and on experimental data from a small-scale automotive application demonstrate the performance of the proposed approach.

Keywords: Non-linear observer design, Lyapunov methods, time-varying systems, water level estimation, air conditioning, automotive test beds, fuel cell test beds.

1. INTRODUCTION

Steam boilers are found in many industrial applications from large-scale boilers used in power plants, see Ahmadi and Toghraie (2016) for an example, down to small-scale boilers used in automotive applications.

One widespread automotive application is the task of air conditioning, i.e. temperature and humidity control, on test beds; in Kancsár et al. (2017), this is done for a fuel cell test bed, for instance (see also Tsotridis et al., 2015). In this context, steam boilers are used to provide steam for humidification. A common control approach for such boilers is on-off control using water level switches and temperature or pressure sensors. This, however, leads to an oscillating behaviour that may affect the actual conditioning task in a negative way. More sophisticated control schemes, such as state feedback control, require the knowledge of temperature and water level. While the former is easily measurable, the latter is not. Thus, an observer may be used to obtain the water level in the boiler.

Although there is literature on the conditioning task itself—see Preglej et al. (2014), Kancsár et al. (2017), Corti et al. (2018), for some recent publications—, little is typically said about steam boiler controllers or observers in these applications. One example for an observer in the context of large-scale steam boilers is found in Marquez and Riaz (2005), who approach the non-linear problem by switching between several linear observers. There also exist several observer concepts for general non-linear systems, see Simon (2006), Adamy (2014), or Pylorof et al. (2019), to name a few examples. These general observers can not exploit the particular structure of the model, however.

In this paper, the steam boiler modelling is revisited with mean density and mean specific internal energy as state variables, instead of the common choice of pressure and water volume (see Åström and Bell, 2000). The model structure thus obtained is then exploited to design an observer that is both easy to implement and to tune. In particular, tuning insight is gained from the fact that its linearised error dynamics are designed to have a (time-varying) oscillator-like structure.

The modelling of steam boilers is discussed in section 2. In section 3, an observer is designed by constructing a Lyapunov function for the linearised error dynamics. In section 4, the closed error dynamics are further analysed to gain insight into observer tuning. Finally, the proposed observer's performance is compared to an extended Kalman filter both in simulation and on experimental data in section 5.

2. MODELLING

Consider the steam boiler depicted in figure 1. Supply water enters at the bottom valve and steam leaves the system at the top valve; the two mass flows shall be denoted by $\dot{m}_{\mathrm{sw}}$ and $\dot{m}_{\mathrm{s}}$, respectively. The water inside the boiler can be heated by means of electric heaters;

⋆ The financial support by the Christian Doppler Research Association, the Austrian Federal Ministry for Digital and Economic Affairs and the National Foundation for Research, Technology and Development is gratefully acknowledged.

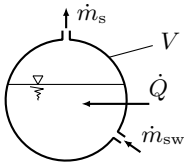

Fig. 1. Schematics of a steam boiler with inner volume V. Supply water enters at the bottom and steam leaves at the top; the heat flow $\dot{Q}$ is produced by means of electric heaters.

the corresponding heat flow shall be denoted by $\dot{Q}$. Note that $\dot{m}_\mathrm{sw}$, $\dot{m}_\mathrm{s}$, and $\dot{Q}$ are non-negative; furthermore it is assumed that they are measurable. Additionally, the steam temperature T_s is measured.

Mass and energy conservation yield

$$\begin{cases} \dfrac{\mathrm{d}m}{\mathrm{d}t} = \dot{m}_\mathrm{sw} - \dot{m}_\mathrm{s}\,, \\ \dfrac{\mathrm{d}(e\cdot m)}{\mathrm{d}t} = \dot{Q} + h_\mathrm{sw}\dot{m}_\mathrm{sw} - h_\mathrm{s}\dot{m}_\mathrm{s}\,, \end{cases} \tag{1}$$

where m is the total mass of water in the system, e the mean specific internal energy, h_sw the specific enthalpy of the supply water, and h_s the specific enthalpy of the steam in the system [1].

It is reasonable (as will be seen later) to choose the mean density ϱ and the mean specific internal energy e as system states; the mean density is explained by the equation $m = \varrho V$, where V is the constant inner volume of the steam boiler. We will regard $\dot{Q}$, $\dot{m}_\mathrm{sw}$, and $\dot{m}_\mathrm{s}$ as system inputs and the steam temperature T_s as system output; thus we may define the vectors

$$\boldsymbol{x} = \begin{bmatrix} x_1 \\ x_2 \end{bmatrix} := \begin{bmatrix} \varrho \\ e \end{bmatrix} \qquad \text{and} \qquad \boldsymbol{u} = \begin{bmatrix} u_1 \\ u_2 \\ u_3 \end{bmatrix} := \begin{bmatrix} \dot{Q} \\ \dot{m}_\mathrm{sw} \\ \dot{m}_\mathrm{s} \end{bmatrix}. \tag{2}$$

If we further assume that vapour and liquid coexist in thermodynamic equilibrium—as is commonly done in steam boiler modelling, see Åström and Bell (2000)—, both T_s and h_s become static functions of the system states and we end up with the final model

$$\frac{\mathrm{d}\boldsymbol{x}}{\mathrm{d}t} = \boldsymbol{f}(\boldsymbol{x},\boldsymbol{u}) = \begin{bmatrix} f_1(\boldsymbol{u}) \\ f_2(\boldsymbol{x},\boldsymbol{u}) \end{bmatrix}, \quad y = g(\boldsymbol{x}) := T_\mathrm{s}(\boldsymbol{x})\,, \tag{3}$$

with

$$f_1(\boldsymbol{u}) := (u_2 - u_3)/V\,, \tag{4}$$

$$f_2(\boldsymbol{x},\boldsymbol{u}) := \frac{u_1 + (h_\mathrm{sw} - x_2)u_2 - (h_\mathrm{s}(\boldsymbol{x}) - x_2)u_3}{V x_1}\,. \tag{5}$$

2.1 Temperature and enthalpy in thermodyn. equilibrium

The assumption of thermodynamic equilibrium has two further implications: first, that temperature is the same everywhere in the boiler and second, that pressure is a function of temperature only and is equal to the saturated vapour pressure, see Gmehling et al. (2012). Hence, water steam tables—such as provided by Wagner and Kruse (1998)—can be used to obtain functional relations between various thermodynamic quantities.

[1] Note that changes in the potential and kinetic energy are negligible, see e.g. Moran and Shapiro (2006).

By choosing ϱ and e as system states, the functional relation between T_s and the system states becomes particularly simple; the same is true for h_s, see figure 2. One can see that both may be approximated by affine functions of the system states:

$$\frac{T_\mathrm{s}}{1\,\mathrm{K}} \approx 274.25 + \frac{1.2925{\cdot}10^{-3}\varrho}{1\,\mathrm{kg/m^3}} + \frac{2.3365{\cdot}10^{-4}e}{1\,\mathrm{J/kg}}\,, \tag{6}$$

$$\frac{h_\mathrm{s}}{1\,\mathrm{J/kg}} \approx 2.5352{\cdot}10^{-6} + \frac{1.9027\varrho}{1\,\mathrm{kg/m^3}} + \frac{0.3332\,e}{1\,\mathrm{J/kg}}\,. \tag{7}$$

The maximum errors introduced by these approximations are $\pm 0.16\,\mathrm{K}$ and $\pm 1.38\,\mathrm{kJ/kg}$ for temperature and enthalpy, respectively.

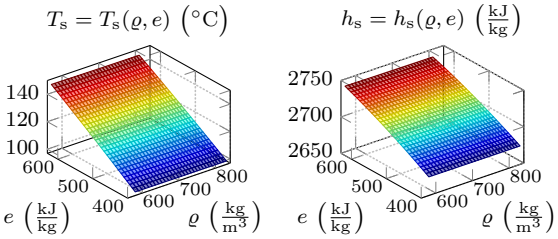

Fig. 2. Steam temperature T_s and specific enthalpy h_s in thermodynamic equilibrium as functions of mean density ϱ and mean specific internal energy e (calculated from water steam tables).

We will thus use the approximations

$$g(\boldsymbol{x}) \approx [c_0\ c_1\ c_2] \begin{bmatrix} 1 \\ x_1 \\ x_2 \end{bmatrix}, \quad h_\mathrm{s}(\boldsymbol{x}) \approx [\eta_0\ \eta_1\ \eta_2] \begin{bmatrix} 1 \\ x_1 \\ x_2 \end{bmatrix}, \tag{8}$$

with c_i, η_i $(i = 0, 1, 2)$ being positive constants, in the above system description, i.e. in (3) and (5).

Remark 1. Note that other properties of the system, such as pressure and water level, are also determined by the chosen system states. The ratio between the water volume V_w and the (constant) inner volume of the boiler V, for instance, may be approximated by

$$\frac{V_\mathrm{w}}{V} \approx \frac{1.0669{\cdot}10^{-3}\varrho}{1\,\mathrm{kg/m^3}} + \frac{1.4905{\cdot}10^{-7}e}{1\,\mathrm{J/kg}} - 7.9223{\cdot}10^{-2}\,. \tag{9}$$

3. OBSERVER DESIGN

Let the observer be a copy of the plant, with the observer state $\hat{\boldsymbol{x}}$ and the observer output $\hat{y}$, plus a correction term, which shall be a time-varying vector [2] $\boldsymbol{\ell}(t)$ times the output error, i.e.

$$\frac{\mathrm{d}\hat{\boldsymbol{x}}}{\mathrm{d}t} = \boldsymbol{f}(\hat{\boldsymbol{x}},\boldsymbol{u}) + \boldsymbol{\ell}(t)\cdot(y - \hat{y})\,, \qquad \hat{y} = g(\hat{\boldsymbol{x}})\,, \tag{10}$$

with $\boldsymbol{\ell}(t) := [\ell_1(t)\ \ell_2(t)]^\mathsf{T}$. The dynamics of the observer error $\boldsymbol{e} := \boldsymbol{x} - \hat{\boldsymbol{x}}$ are

$$\begin{aligned} \frac{\mathrm{d}\boldsymbol{e}}{\mathrm{d}t} &= \boldsymbol{f}(\boldsymbol{x},\boldsymbol{u}) - \boldsymbol{f}(\hat{\boldsymbol{x}},\boldsymbol{u}) - \boldsymbol{\ell}(t)\cdot(y - \hat{y}) \\ &= \begin{bmatrix} -\ell_1(t)\cdot\big(g(\boldsymbol{x}) - g(\hat{\boldsymbol{x}})\big) \\ f_2(\boldsymbol{x},\boldsymbol{u}) - f_2(\hat{\boldsymbol{x}},\boldsymbol{u}) - \ell_2(t)\cdot\big(g(\boldsymbol{x}) - g(\hat{\boldsymbol{x}})\big) \end{bmatrix}. \end{aligned} \tag{11}$$

In the following, $\boldsymbol{\ell}(t)$ is designed such that the error dynamics are (locally) asymptotically stable. To that end, (11) will be linearised.

[2] Time dependency will be explicitly stated, except for state variables where it is omitted for the sake of simplicity.

3.1 Linearised, time-varying error dynamics

The function f_2 may be expressed by a Taylor series in the observer state $\hat{\boldsymbol{x}}$; for small errors $\boldsymbol{e}$ it is thus approximated by

$$f_2(\boldsymbol{x},\boldsymbol{u}) \approx f_2(\hat{\boldsymbol{x}},\boldsymbol{u}) + \left.\frac{\partial f_2}{\partial \boldsymbol{x}}\right|_{\hat{\boldsymbol{x}},\boldsymbol{u}} \cdot \boldsymbol{e}\,. \tag{12}$$

The same can be done with the output function $g(\boldsymbol{x})$; hence, the error dynamics may be approximated by the linear, time-varying system

$$\frac{\mathrm{d}\boldsymbol{e}}{\mathrm{d}t} \approx (\boldsymbol{A}(t) - \boldsymbol{\ell}(t)\boldsymbol{c}(t)^\mathsf{T})\,\boldsymbol{e}\,, \tag{13}$$

where $\boldsymbol{A}(t)$ has the special structure

$$\boldsymbol{A}(t) := \begin{bmatrix} \boldsymbol{0}^\mathsf{T} \\ \partial f_2/\partial \boldsymbol{x}|_{\hat{\boldsymbol{x}},\boldsymbol{u}} \end{bmatrix} = \begin{bmatrix} 0 & 0 \\ a_1(t) & a_2(t) \end{bmatrix} \tag{14}$$

and $\boldsymbol{c}(t) := (\partial g/\partial \boldsymbol{x}|_{\hat{\boldsymbol{x}}})^\mathsf{T}$. Using (8), we find that $\boldsymbol{c}(t)$ becomes a constant vector with $\boldsymbol{c} = [c_1\ c_2]^\mathsf{T}$; furthermore we find

$$a_1(t) = q_1(\hat{\boldsymbol{x}}(t),\boldsymbol{u}(t)) \quad \text{and} \quad a_2(t) = q_2(\hat{\boldsymbol{x}}(t),\boldsymbol{u}(t)) \tag{15}$$

with

$$q_1(\boldsymbol{x},\boldsymbol{u}) := -\frac{u_1 + (h_\mathrm{sw} - x_2)u_2 - (\eta_0 + (\eta_2 - 1)x_2)u_3}{V x_1^2}\,, \tag{16}$$

$$q_2(\boldsymbol{x},\boldsymbol{u}) := -\frac{u_2 + (\eta_2 - 1)u_3}{V x_1}\,. \tag{17}$$

3.2 Lyapunov-based design

In the following, a Lyapunov function is used to find suitable observer gains $\ell_1(t)$ and $\ell_2(t)$. To that end, the state transformation

$$\boldsymbol{z} = \boldsymbol{T}\boldsymbol{e} \qquad \text{with} \qquad \boldsymbol{T} = \begin{bmatrix} 1 & 0 \\ c_1/c_2 & 1 \end{bmatrix} \tag{18}$$

is introduced, which yields the transformed error dynamics

$$\frac{\mathrm{d}\boldsymbol{z}}{\mathrm{d}t} = \underbrace{\boldsymbol{T}(\boldsymbol{A}(t) - \boldsymbol{\ell}(t)\boldsymbol{c}^\mathsf{T})\boldsymbol{T}^{-1}}_{=:\boldsymbol{\Lambda}(t)}\boldsymbol{z} = \boldsymbol{\Lambda}(t)\boldsymbol{z}\,, \tag{19}$$

where

$$\boldsymbol{\Lambda}(t) = \begin{bmatrix} 0 & -\ell_1(t)c_2 \\ \tilde{a}_1(t) & a_2(t) - \tilde{\ell}_2(t)c_2 \end{bmatrix} \tag{20}$$

with

$$\tilde{a}_1(t) = a_1(t) - a_2(t)\frac{c_1}{c_2}\,, \quad \tilde{\ell}_2(t) = \ell_2(t) + \ell_1(t)\frac{c_1}{c_2}\,. \tag{21}$$

With (16) and (17), we may define

$$\tilde{q}_1(\boldsymbol{x},\boldsymbol{u}) := q_1(\boldsymbol{x},\boldsymbol{u}) - \frac{c_1}{c_2}q_2(\boldsymbol{x},\boldsymbol{u})\,, \tag{22}$$

which is equal to $\tilde{a}_1(t)$ if evaluated at the observer state, i.e. $\tilde{a}_1(t) = \tilde{q}_1(\hat{\boldsymbol{x}}(t),\boldsymbol{u}(t))$; this definition will be useful later.

Notice in (20) that the time derivative of z_1 is not influenced by z_1 but only by z_2; this will be exploited in the following.

Consider the positive definite function

$$U(\boldsymbol{z}) = \frac{1}{2}(z_1^2 + \alpha z_2^2) \quad \text{with} \quad \alpha = \text{const.} > 0\,. \tag{23}$$

Its time derivative along the trajectories of $\boldsymbol{z}$ is

$$\dot{U} = (\alpha\tilde{a}_1(t) - \ell_1(t)c_2)z_1 z_2 + \alpha(a_2(t) - \tilde{\ell}_2(t)c_2)z_2^2\,. \tag{24}$$

By choosing $\ell_1(t) = \alpha\tilde{a}_1(t)/c_2$, we get

$$\dot{U} = \alpha(a_2(t) - \tilde{\ell}_2(t)c_2)z_2^2\,. \tag{25}$$

If the inequality $a_2(t) - \tilde{\ell}_2(t)c_2 < 0$ is satisfied, $\dot{U}$ is negative semi-definite. Thus, we introduce a positive constant [3] ζ and choose

$$\tilde{\ell}_2(t) = \frac{a_2(t) + \zeta}{c_2}\,, \tag{26}$$

which finally yields $\dot{U} = -\alpha\zeta z_2^2$. As $\dot{U}$ is negative semi-definite, U is a Lyapunov function. If we insert the so chosen $\ell_1(t)$ and $\tilde{\ell}_2(t)$ into (20), we get the transformed error dynamics

$$\frac{\mathrm{d}\boldsymbol{z}}{\mathrm{d}t} = \begin{bmatrix} 0 & -\alpha\tilde{a}_1(t) \\ \tilde{a}_1(t) & -\zeta \end{bmatrix}\boldsymbol{z}\,, \tag{27}$$

which corresponds to a damped oscillator (see section 4). To sum up, by the choice

$$\ell_1(t) = \alpha\frac{\tilde{a}_1(t)}{c_2}\,, \qquad \ell_2(t) = \frac{a_2(t) + \zeta - c_1\ell_1(t)}{c_2}\,, \tag{28}$$

stability of the linear, time-varying system (19) is ensured; this implies stability of the linearised system (13).

3.3 Observer convergence

In the previous section, we considered the linearised system (13); however, we still have to show that the original, non-linear observer converges. As the time derivative of U is only negative semi-definite, we can not conclude that the non-linear observer converges. We will thus construct a strict Lyapunov function [4] for (27) to show local stability of the original, non-linear observer.

Theorem 2. Consider the non-linear, time-varying observer (10) with gains $\ell_1(t)$, $\ell_2(t)$ chosen according to (28). If the sign of $\tilde{a}_1(t)$ is constant and $\epsilon \le 2|\tilde{a}_1(t)|\sqrt{\alpha}/\zeta \le 1/\epsilon$ holds for some $\epsilon > 0$ and all t, then the origin of its error dynamics (11) is (locally) asymptotically stable.

Proof. Similar to the approach in Cruz-Zavala et al. (2018), we introduce a modified Lyapunov function

$$W(\boldsymbol{z}) = U(\boldsymbol{z}) - \beta z_1 z_2 = \frac{1}{2}\boldsymbol{z}^\mathsf{T}\begin{bmatrix} 1 & -\beta \\ -\beta & \alpha \end{bmatrix}\boldsymbol{z}\,, \tag{29}$$

where β is a non-zero constant chosen such that W is positive definite, i.e. $\beta^2 < \alpha$. The time derivative of W along the trajectories of $\boldsymbol{z}$ is

$$\dot{W} = -\boldsymbol{z}^\mathsf{T}\begin{bmatrix} \beta\tilde{a}_1(t) & -\beta\zeta/2 \\ -\beta\zeta/2 & \alpha\big(\zeta - \beta\tilde{a}_1(t)\big) \end{bmatrix}\boldsymbol{z}\,, \tag{30}$$

which is negative definite, if both

$$\beta\tilde{a}_1(t) \ge \delta_1 > 0 \qquad \text{and} \tag{31}$$

$$-(\alpha[\tilde{a}_1(t)]^2 + \zeta^2/4)\beta^2 + \alpha\tilde{a}_1(t)\zeta\beta \ge \delta_2 > 0 \tag{32}$$

hold for some δ_1, δ_2. By choosing

$$\beta = \sqrt{\alpha}\frac{\epsilon}{1 + (1/\epsilon)^2} \cdot \operatorname{sgn}\tilde{a}_1(t)\,, \tag{33}$$

it can be shown that some δ_1, δ_2 exist (see appendix A); thus W is a strict Lyapunov function [5] and we can conclude that the origin of the non-linear observer error dynamics is (locally) asymptotically stable. □

[3] Of course, ζ may also be a function of time.

[4] We call a Lyapunov function *strict*, if its time derivative is negative definite.

[5] Note that $\beta^2 < \alpha$ is true if $\epsilon^3/(1 + \epsilon^2) < 1$ holds, i.e. for small ϵ.

Remark 3. Theorem 2 requires a constant sign of $\tilde{a}_1(t)$. If it does change sign, however, local asymptotic stability may still be guaranteed, in a similar way as is done in Branicky (1998) or Geromel and Colaneri (2006). The idea is to switch the Lyapunov function by changing the sign of β, as $\tilde{a}_1(t)$ changes sign. This may lead to a positive step-wise change in W, yet if $\tilde{a}_1(t)$ does not change sign again for some (sufficiently large) minimum dwell-time, W will still decay and thus, the origin is still (locally) asymptotically stable. This works provided that the sign of $\tilde{a}_1(t)$ does not change too frequently—a reasonable assumption, as $\tilde{a}_1(t)$ depends on the input (see next chapter).

The case $\tilde{a}_1(t) = 0$ will be addressed in the following section.

3.4 Observability

As we have seen in the previous section, $\tilde{a}_1(t)$ plays an important role for observer convergence. It will be shown in this section that it is also related to the so-called weak observability.

Weak observability is understood in the sense that a system's unknown initial state $\boldsymbol{x}_0$ is uniquely determinable in a *neighbourhood* of $\boldsymbol{x}_0$ from the knowledge of its inputs and outputs in a finite time interval. This has to be true everywhere in the state space for the system to be called weakly observable. The concept of weak observability and the sufficient condition to show it follow Adamy (2014); the idea behind the sufficient condition is also found in Isidori (1995).

Given the system (3), let $\bar{\boldsymbol{y}}$ be a vector consisting of the output and its first time derivative, i.e.

$$\bar{\boldsymbol{y}} := [y \quad \mathrm{d}y/\mathrm{d}t]^\mathsf{T}. \tag{34}$$

The vector $\bar{\boldsymbol{y}}$ may be expressed as a function of $\boldsymbol{x}$ and $\boldsymbol{u}$, i.e.

$$\bar{\boldsymbol{y}} = \boldsymbol{t}(\boldsymbol{x}, \boldsymbol{u}), \tag{35}$$

which may be interpreted as a coordinate transformation. Now, if a unique inverse function $\boldsymbol{\tau}$ exists (at least locally) such that

$$\boldsymbol{x} = \boldsymbol{\tau}(\bar{\boldsymbol{y}}, \boldsymbol{u}), \tag{36}$$

then, the system is weakly observable. According to the implicit function theorem, $\boldsymbol{\tau}$ locally exists, if

$$\det \frac{\partial \boldsymbol{t}}{\partial \boldsymbol{x}} \neq 0. \tag{37}$$

As $\boldsymbol{t}$ is given by

$$\boldsymbol{t}(\boldsymbol{x}, \boldsymbol{u}) = \begin{bmatrix} c_0 + \boldsymbol{c}^\mathsf{T}\boldsymbol{x} \\ c_1 f_1(\boldsymbol{u}) + c_2 f_2(\boldsymbol{x}, \boldsymbol{u}) \end{bmatrix}, \tag{38}$$

one finds that

$$\det \frac{\partial \boldsymbol{t}}{\partial \boldsymbol{x}} = \det \begin{bmatrix} \boldsymbol{c}^\mathsf{T} \\ c_2(\partial f_2/\partial \boldsymbol{x}) \end{bmatrix} = -c_2^2\, \tilde{q}_1(\boldsymbol{x}, \boldsymbol{u}), \tag{39}$$

with $\tilde{q}_1$ as defined in (22). Remember that if $\tilde{q}_1(\boldsymbol{x}, \boldsymbol{u})$ is evaluated at $\hat{\boldsymbol{x}}$, it becomes $\tilde{a}_1(t)$; thus, $\tilde{a}_1(t)$ is closely related to observability, especially if the observer error is small. The function $\tilde{q}_1(\boldsymbol{x}, \boldsymbol{u})$ takes on the form

$$\tilde{q}_1(\boldsymbol{x}, \boldsymbol{u}) = \frac{1}{V x_1^2} \boldsymbol{\varphi}(\boldsymbol{x})^\mathsf{T} \boldsymbol{u}, \tag{40}$$

with

$$\boldsymbol{\varphi}(\boldsymbol{x}) := [-1 \quad \xi - h_\mathrm{sw} \quad \eta_0 + (\eta_2 - 1)\xi]^\mathsf{T}, \quad \xi := x_1 c_1/c_2 + x_2. \tag{41}$$

So we end up with the sufficient condition: if $\boldsymbol{\varphi}(\boldsymbol{x})^\mathsf{T}\boldsymbol{u} \neq 0$, then (3) is weakly observable.

As $\tilde{a}_1(t) \neq 0$ is important for both observability and observer convergence, we will henceforth assume that $\tilde{a}_1(t)$ does not vanish. This has to be ensured by a proper choice of $\boldsymbol{u}$.

4. TUNING RULES

In order to gain more insight into the error dynamics, we introduce another state transformation from the states z_1 and z_2 to the states U (which is the Lyapunov function from above) and θ, where the transformation is given by

$$\boldsymbol{z} = U \cdot \begin{bmatrix} \cos(\theta/2) \\ \dfrac{1}{\sqrt{\alpha}} \sin(\theta/2) \end{bmatrix}. \tag{42}$$

This transformation is motivated by the fact that (27) corresponds to a damped oscillator; the transformed system may be interpreted as some kind of polar representation, only that for constant U, we get ellipses instead of circles in the (z_1, z_2)-plane in general.

According to the chain rule of differentiation, we get

$$\frac{\mathrm{d}\boldsymbol{z}}{\mathrm{d}t} = \begin{bmatrix} \cos(\theta/2) & -U\sin(\theta/2) \\ \dfrac{1}{\sqrt{\alpha}}\sin(\theta/2) & \dfrac{U}{\sqrt{\alpha}}\cos(\theta/2) \end{bmatrix} \begin{bmatrix} \mathrm{d}U/\mathrm{d}t \\ \mathrm{d}(\theta/2)/\mathrm{d}t \end{bmatrix}. \tag{43}$$

Using (27), we end up with

$$\begin{cases} \dfrac{\mathrm{d}U}{\mathrm{d}t} = -U\dfrac{\zeta}{2}(1 - \cos\theta), \\ \dfrac{\mathrm{d}\theta}{\mathrm{d}t} = 2\tilde{a}_1(t)\sqrt{\alpha} - \zeta \sin\theta. \end{cases} \tag{44}$$

According to the first equation, $|U|$ decreases as long as $(1 - \cos\theta) \neq 0$. Furthermore, the decay rate is influenced by the term $(1 - \cos\theta)$; thus, the behaviour of θ shall be further analysed. The second equation of (44) may be rewritten as

$$\frac{\mathrm{d}\theta}{\mathrm{d}t} = 2|\tilde{a}_1(t)|\sqrt{\alpha} \cdot \left(\operatorname{sgn}\tilde{a}_1(t) - \frac{\zeta}{2|\tilde{a}_1(t)|\sqrt{\alpha}} \sin\theta \right). \tag{45}$$

Notice from this representation that $\tilde{a}_1(t)$ may be interpreted as the oscillator's frequency; thus, it is intuitive why $\tilde{a}_1(t) \neq 0$ is required for the observer to converge in general.

We are interested in possible equilibria of θ. To simplify our considerations, we will let ζ be

$$\zeta(t) = \psi \cdot 2|\tilde{a}_1(t)|\sqrt{\alpha}, \tag{46}$$

with some constant ψ. Equilibria θ_eq may be obtained by solving

$$\sin\theta_\mathrm{eq} \overset{!}{=} \frac{2|\tilde{a}_1(t)|\sqrt{\alpha}}{\zeta(t)} \operatorname{sgn}\tilde{a}_1(t) = \frac{1}{\psi} \operatorname{sgn}\tilde{a}_1(t). \tag{47}$$

Here, we can distinguish two cases:

Case 1. $\psi < 1$. In this case, (47) has no solution; this implies $\mathrm{d}\theta/\mathrm{d}t \not\equiv 0$ and thus

$$(1 - \cos\theta) \not\equiv 0. \tag{48}$$

So U certainly tends to zero, but with an oscillating behaviour. We may call this case "*underdamped*" in allusion to time-invariant second order systems.

Case 2. $\psi \geq 1$. In this case, solutions of (47) exist; however, for given ψ and sign of $\tilde{a}_1(t)$, we get two solutions in the interval $[-\pi, \pi]$ in general. Figure 3 shows these two equilibria for positive $\tilde{a}_1(t)$; if $\tilde{a}_1(t)$ is negative, the figure is basically the same if θ is replaced by $-\theta$, since $\sin\theta$ is an odd function. We can conclude from figure 3 that θ will reach equilibrium—if $\tilde{a}_1(t)$ does not change sign—and once in equilibrium, U will decay exponentially without oscillations.

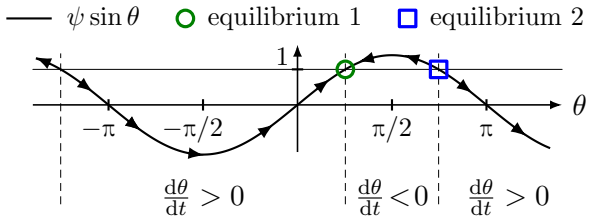

Fig. 3. Two equilibria in the interval $[-\pi, \pi]$ for positive $\tilde{a}_1(t)$ and $\psi > 1$; these equilibria are periodic with period 2π. As can be seen by the sign of $\mathrm{d}\theta/\mathrm{d}t$ and as indicated by the arrows, equilibrium 1 (green circle) is asymptotically stable; equilibrium 2 (blue square) is unstable.

Further notice that in equilibrium 1, $\cos\theta_{\mathrm{eq}}$ will be positive and the closer to 1, the larger ψ is; yet this means that the decay rate of U gets smaller, the larger ψ gets. Thus, we may call this case "*overdamped*". The fastest decay of U is obtained for $\psi = 1$, which is just the border case that may be called "*critically damped*".

Now, let us turn back to ζ being constant. Of course, this implies that ψ is not constant but changes with $\tilde{a}_1(t)$; thus, equilibria of θ may change as well. However, we may still distinguish between $\psi(t) < 1$ and $\psi(t) \geq 1$, as the principal behaviour in these two cases stays the same.

Having studied those two cases, it is reasonable to choose ζ such that the system is in the "overdamped" case, possibly close to the "critical" case, to prevent excessive oscillations while maintaining a good convergence speed. As ζ is thus determined, the only remaining parameter is α, which corresponds to the "observer speed".

5. SIMULATION AND EXPERIMENTAL RESULTS

The proposed observer is tested both in simulation and on experimental data. To that end, (10) was implemented using the observer gains proposed in (28). The tuning was done empirically according to the rules given in section 4. In addition, an extended Kalman filter was implemented for the sake of comparison; it was also tuned empirically [6].

For the experimental data, the steam boiler depicted in figure 4 was operated in different operating regions; the simulations were done with a model of this steam boiler.

The depicted boiler is used in an air conditioning application for automotive test beds. It can be operated to a maximum absolute pressure of $4{\cdot}10^5$ Pa (a safety valve opens beyond this point). The two water level switches are used for safety reasons to ensure that the electrical heaters

[6] For details on implementation and tuning of an extended Kalman filter, see Simon (2006) or Adamy (2014).

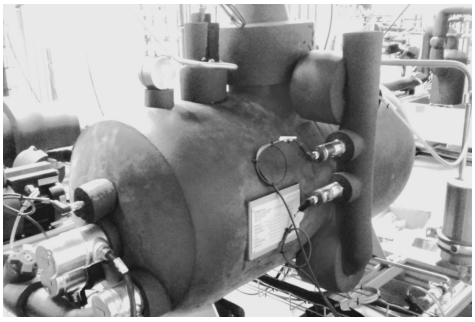

Fig. 4. An insulated steam boiler with a volume of about a hundred litre. Three of the electrical heaters can be seen at the bottom left; above the heaters is a temperature sensor. Two water level switches are mounted at the vertical pipe in the middle.

are always covered with water and to restrain the water level to a certain maximum. The six electrical heaters can provide a heat flow of 54 kW in total. The steam valve's nominal size is DN 15, leading to a maximum steam mass flow of about $80{\cdot}10^{-4}$ kg/s at the maximum absolute pressure.

5.1 Simulation

For the simulation, steam mass flow and heat flow are chosen as shown in figure 5; supply water was not used.

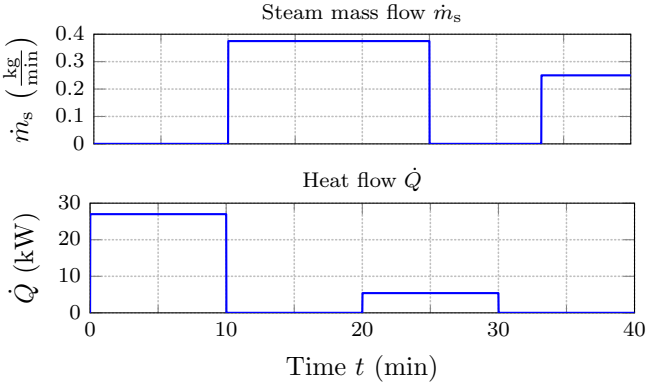

Fig. 5. Steam mass flow $\dot{m}_{\mathrm{s}}$ and heat flow $\dot{Q}$ used in simulation.

As the steam temperature is mainly influenced by the specific internal energy e and scarcely by the density ϱ (see (6) and figure 2), it may be used to initialise the observer. If the density is chosen in the middle of the interesting region (i.e. 600 kg/m^3 to 800 kg/m^3), the maximum error for e in the interesting region (i.e. 400 kJ/kg to 600 kJ/kg) is only ± 0.55 kJ/kg—if calculated according to (6). The internal energy was initialised in this way using (6). The initial density error was in fact chosen larger to demonstrate a larger region of attraction.

Figure 6 shows one simulation result; notice that even though the initial density error is quite large, the observer converges. The proposed observer and the extended Kalman filter show comparable results; however, the proposed observer required less implementation and tuning effort.

The corresponding $\tilde{a}_1(t)$ and $\tilde{q}_1(\boldsymbol{x}, \boldsymbol{u})$ are shown in figure 7. One can see that these two are practically the same as soon as the observer error is small. Further notice that, in this example, the system is weakly observable as long as there is some input to the system.

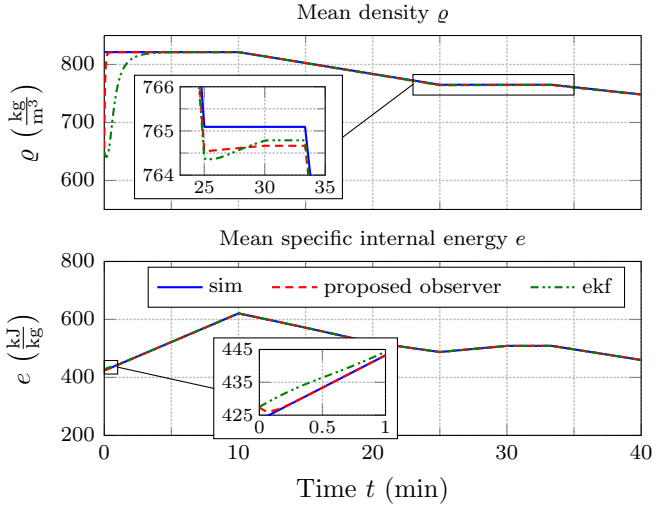

Fig. 6. Simulation results for the proposed observer and the extended Kalman filter (ekf); tuning of the proposed observer: $\zeta = 1.5\sqrt{\alpha}$, $\alpha = 2.5{\cdot}10^{-2}$.

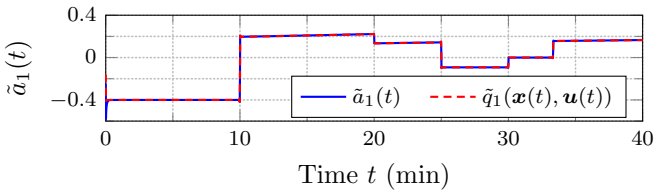

Fig. 7. Functions $\tilde{a}_1(t)$ as defined by (21) and $\tilde{q}_1(\boldsymbol{x}, \boldsymbol{u})$ as given in (40) for the previously shown simulation.

To illustrate the influence of ζ, figure 8 shows the observer error for the same simulation, but with different ζ. The typical behaviour in the "under"- and "overdamped" case is clearly seen. The best result, however, was obtained for a constant ζ in combination with a larger α. In the constant case, ζ was chosen such that the system is "overdamped". As suggested in section 4, this case shows the typical behaviour of the "overdamped" case, i.e. no strong oscillations, even though ζ is constant.

5.2 Experimental data

As said before, the boiler is equipped with two water level switches. As the position of these switches is known, the system states can be calculated quite accurately when the water level reaches a level switch. The experiment was thus conducted such that the water level decreased from the upper level at time t_0 to the lower level at time t_1; the results are shown in figure 9. The observer was initialised with the calculated states at t_0.

It can be seen in figure 9 that the mean density at time t_1 matches quite well with the calculated value ϱ_1 for both the proposed observer and the extended Kalman filter; the variations are due to model uncertainties and a

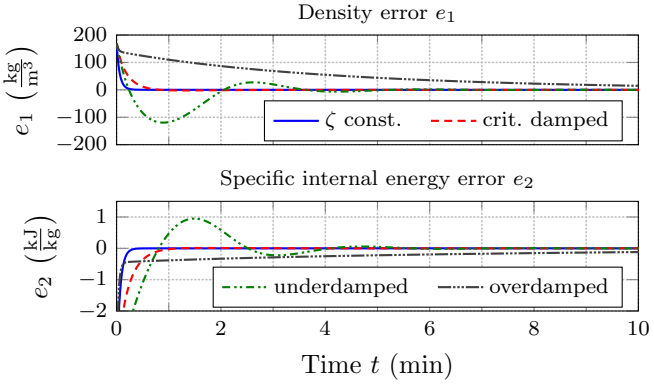

Fig. 8. The case "ζ const." is the same as shown before. The other three cases have $\zeta(t) = \psi \cdot 2|\tilde{a}_1(t)|\sqrt{\alpha}$ and $\alpha = 8{\cdot}10^{-3}$ with $\psi = 1$ for "crit. damped", $\psi = 0.3$ for "underdamped", and $\psi = 5$ for "overdamped".

matter of tuning. The proposed observer is comparable in performance to the extended Kalman filter at a reduced implementation complexity and an intuitive tuning perspective.

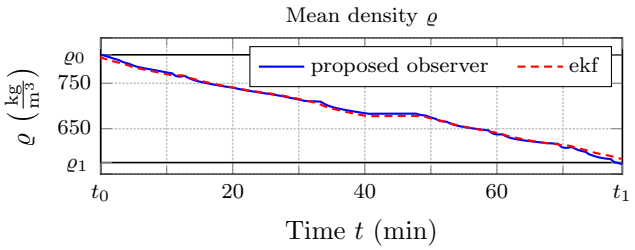

Fig. 9. Experimental results for the proposed observer and the extended Kalman filter (ekf). At time t_0, the water level is at the upper level switch and the mean density at this point is ϱ_0; likewise, the water level is at the lower level switch at time t_1 and the mean density at this point is ϱ_1.

6. CONCLUSION

The task of constructing an observer for steam boilers was considered. To that end, mean density and mean specific internal energy were chosen as the boiler model's state variables. This has the advantage that all relevant thermodynamic quantities can be approximated by affine functions of these variables and that the linearised observer error dynamics can be designed to be a time-varying, second order oscillator. By means of a polar representation of this oscillator, valuable tuning insight was obtained. Simulations and experiments on a small-scale boiler for an automotive application showed that the proposed observer's performance is comparable to an extended Kalman filter at a reduced implementation and tuning effort.

REFERENCES

Adamy, J. (2014). *Nichtlineare Systeme und Regelungen*. Springer, Berlin Heidelberg, second edition. (In German).

Ahmadi, G.R. and Toghraie, D. (2016). Energy and exergy analysis of Montazeri steam power plant in Iran.

Renewable and Sustainable Energy Reviews, 56, 454–463.

Åström, K.J. and Bell, R.D. (2000). Drum-boiler dynamics. *Automatica*, 36(3), 363–378.

Branicky, M.S. (1998). Multiple Lyapunov functions and other analysis tools for switched and hybrid systems. *IEEE Transactions on automatic control*, 43(4), 475–482.

Corti, E., Taccioli, M., and Ravaglioli, V. (2018). Model-based control of test bench conditioning systems. *SAE International Journal of Engines*, 11(6), 1195–1208.

Cruz-Zavala, E., Sanchez, T., Moreno, J.A., and Nuño, E. (2018). Strict Lyapunov functions for homogeneous finite-time second-order systems. In *2018 Conference on Decision and Control (CDC)*, 1530–1535. IEEE.

Geromel, J.C. and Colaneri, P. (2006). Stability and stabilization of continuous-time switched linear systems. *SIAM Journal on Control and Optimization*, 45(5), 1915–1930.

Gmehling, J., Kolbe, B., Kleiber, M., and Rarey, J. (2012). *Chemical Thermodynamics for Process Simulation*. Wiley-VCH, Weinheim.

Isidori, A. (1995). *Nonlinear control systems*. Springer, Berlin Heidelberg New York, third edition.

Kancsár, J., Striednig, M., Aldrian, D., Trattner, A., Klell, M., Kügele, C., and Jakubek, S. (2017). A novel approach for dynamic gas conditioning for PEMFC stack testing. *International journal of hydrogen energy*, 42(48), 28898–28909.

Marquez, H.J. and Riaz, M. (2005). Robust state observer design with application to an industrial boiler system. *Control Engineering Practice*, 13(6), 713–728.

Moran, M.J. and Shapiro, H.N. (2006). *Fundamentals of Engineering Thermodynamics*. John Wiley & Sons Ltd, Chichester, fifth edition.

Preglej, A., Rehrl, J., Schwingshackl, D., Steiner, I., Horn, M., and Škrjanc, I. (2014). Energy-efficient fuzzy model-based multivariable predictive control of a HVAC system. *Energy and Buildings*, 82, 520–533.

Pylorof, D., Bakolas, E., and Chan, K.S. (2019). Design of robust Lyapunov-based observers for nonlinear systems with sum-of-squares programming. *IEEE Control Systems Letters*, 4(2), 283–288.

Simon, D. (2006). *Optimal state estimation: Kalman, H infinity, and nonlinear approaches*. John Wiley & Sons, Inc, New Jersey.

Tsotridis, G., Pilenga, A., De Marco, G., and Malkow, T. (2015). EU harmonised test protocols for PEMFC MEA testing in single cell configuration for automotive applications. *JRC Science for Policy report*, EUR 27632 EN.

Wagner, W. and Kruse, A. (1998). *Properties of Water and Steam: The Industrial Standard IAPWS-IF97 for the Thermodynamic Properties and Supplementary Equations for Other Properties*. Springer, Berlin Heidelberg.

Appendix A. EXISTENCE OF δ_1, δ_2

In the following,

$$\epsilon \leq \frac{2|\tilde{a}_1(t)|\sqrt{\alpha}}{\zeta} \leq 1/\epsilon \tag{A.1}$$

and

$$\beta = \frac{\sqrt{\alpha}\epsilon}{1+(1/\epsilon)^2} \cdot \operatorname{sgn} \tilde{a}_1(t) \tag{A.2}$$

are employed without being mentioned. Furthermore,

$$\psi(t) := \frac{\zeta}{2|\tilde{a}_1(t)|\sqrt{\alpha}} \tag{A.3}$$

is introduced for the sake of simplicity. Observe that both

$$\epsilon \leq \frac{1}{\psi(t)} \leq \frac{1}{\epsilon} \qquad \text{and} \qquad \epsilon \leq \psi(t) \leq \frac{1}{\epsilon} \tag{A.4}$$

hold.

Existence of δ_1:

$$\begin{aligned} \beta\tilde{a}_1(t) &= \frac{\sqrt{\alpha}\epsilon}{1+(1/\epsilon)^2}|\tilde{a}_1(t)| \geq \frac{\sqrt{\alpha}\epsilon}{1+(1/\epsilon)^2}\frac{\zeta}{2\sqrt{\alpha}}\epsilon \\ &= \frac{\zeta}{2}\frac{\epsilon^2}{1+(1/\epsilon)^2} = \frac{\zeta}{2}\frac{\epsilon^4}{1+\epsilon^2} = \delta_1 > 0\,. \end{aligned} \tag{A.5}$$

Existence of δ_2:

$$\begin{aligned} &-(\alpha[\tilde{a}_1(t)]^2 + \zeta^2/4)\beta^2 + \alpha\tilde{a}_1(t)\zeta\beta \\ &\quad= \big[-(\alpha|\tilde{a}_1(t)|^2 + \zeta^2/4)|\beta| + \alpha|\tilde{a}_1(t)|\zeta\big]|\beta| \\ &\quad= \left[-\alpha|\tilde{a}_1(t)|^2(1+[\psi(t)]^2)\frac{\sqrt{\alpha}\epsilon}{1+(1/\epsilon)^2} + \alpha|\tilde{a}_1(t)|\zeta\right]|\beta| \\ &\quad= \alpha^{\frac{3}{2}}|\tilde{a}_1(t)|^2 2\Bigg[-\frac{\epsilon}{2}\underbrace{\frac{1+[\psi(t)]^2}{1+(1/\epsilon)^2}}_{\leq 1} + \underbrace{\psi(t)}_{\geq\epsilon}\Bigg]\frac{\sqrt{\alpha}\epsilon}{1+(1/\epsilon)^2} \\ &\quad\geq \alpha^{\frac{3}{2}}|\tilde{a}_1(t)|^2\epsilon\frac{\sqrt{\alpha}\epsilon}{1+(1/\epsilon)^2} = \alpha^2|\tilde{a}_1(t)|^2\frac{\epsilon^2}{1+(1/\epsilon)^2} \\ &\quad\geq \alpha^2\frac{\zeta^2}{4\alpha}\frac{\epsilon^4}{1+(1/\epsilon)^2} = \alpha\frac{\zeta^2}{4}\frac{\epsilon^6}{1+\epsilon^2} = \delta_2 > 0\,. \end{aligned} \tag{A.6}$$